

Flow Profiles and Directionality in Microcapillaries Measured by Fluorescence Correlation Spectroscopy

P.-F. Lenne, D. Colombo, H. Giovannini and H. Rigneault

Institut Fresnel UMR CNRS 6133, ENSPM
Domaine Universitaire de St Jérôme
13397 Marseille Cedex 20
France

Correspondence to

P.-F. Lenne

Institut Fresnel UMR CNRS 6133, ENSPM, Domaine
Universitaire de St Jérôme, 13397 Marseille Cedex 20,
France

tel *33 (0) 491 28 80 49

fax *33 (0) 491 28 80 67

email lenne@fresnel.fr or herve.rigneault@fresnel.fr

submitted 29 Apr 2002

accepted 30 Jun 2002

published 10 Jul 2002

keywords: microfluidics, fluorescence correlation spectroscopy, flow profiles

Abstract

We report hydrodynamic and electrophoretic flow profiling in microcapillaries using fluorescence correlation spectroscopy. We find that capillary electrophoresis results in various velocity profiles depending on capillary diameter - constant in small capillaries and parabolic in large ones-, while hydrodynamic flow velocity profile is Poiseuille like. The deviation from the expected electrophoretic constant flow profile in large

capillaries is attributed to thermal effect. Furthermore, we propose and demonstrate a new method for flow directionality measurement using a non-symmetric transverse excitation beam profile.

Introduction

Optical detection of single molecule in solution has become more and more important for many applications ranging from molecular diagnostic [1], such as DNA sequencing [2,3] and immunoassays [2,3], to high-throughput screening (HTS) [6]. Although fluorescence techniques have undoubtedly extended their range of application down to the single molecule level [7], there is still a challenge in a quick monitoring of a single molecular interaction in a well restricted and control environment. To achieve such a task one needs an ultra-sensitive technique to perform single molecule detection (SMD) together with an etching technology to build micro-size structures. Such association would increase throughput, conserve reagent and lower the screening costs.

Concerning miniaturisation, capillary gel electrophoresis was the first technique implemented to achieve DNA sequencing and was quickly extended to single-lane microfabricated device for the analysis of DNA restriction fragments [8]. Pushing further out the technology leads now to Lab-on-a-chip [9] which gathers valves, pressure systems, reactions chambers and detection system on the same micron-size substrate. Such a device has the potential to shrink a room full instruments into a compact and handy chip. As an example, multiplex systems with up to 96 different sample inlets have been developed [10] for rapid analysis of

PCR products. Once the technological fabrication problems are solved, the difficulty is shifted to microfluidic monitoring which can be solved using pressure flow with valves or electrophoretic flow. These flows are important to control accurately both in space and time.

Whereas most of these microfluidics-assays detect burst of photons that correspond to a large number of molecules, SMD techniques are able to detect in routine single molecule events. Fluorescence Correlation Spectroscopy (FCS) [11] is one of these mature technology which can detect single molecule diffusing in and out of a collection volume which can be as small as 1 fl (10^{-15} l). Although single molecule counting and identification have been reported in microcapillaries [12], FCS and especially its commercial implementation have been mostly restricted to open volume [13]. This is the case in HTS implementation [14-16].

There are relatively few published examples of flow profiling in microcapillaries and amongst them FCS has proven valuable for pressure flow profiling measurement in microstructures [17].

We demonstrate here that FCS can determine a variety of flow profiles that are commonly driven in microfabricated capillaries. FCS has the double advantage to use low concentration of markers and gives high-resolution profiling. In this paper, we implement the FCS technique in glass capillaries of various diameters to measure (1) the hydrodynamic and electrophoretic flow profiles and their possible variation with temperature and (2) the flow directionality.

These results show that FCS can be used as a characterisation technique to accurately monitor microfluidic flows in any HTS or micro-system framework.

Theory

Fluorescence Correlation Spectroscopy with Translational Flow

Fluorescence correlation spectroscopy is the analysis of fluctuations in intensity of individual molecules in a very small (\sim fl) and open volume [18]. The transverse and axial dimensions of this volume are generally defined by a laser beam focused by an high numerical aperture objective, and a confocal pinhole which sets the fraction of light collected by the detectors. We consider both cases of circular and elliptic laser beam cross-section and define w_x and w_y as the two axis lengths of the ellipsoidal laser cross-section at the focal plane of the objective. z_0 stands for the axial size of the collection volume (see figure 1).

The intensity fluctuations $\delta i(t) = i(t) - \langle i \rangle$, where $i(t)$ is the detected fluorescence intensity and $\langle \rangle$ stands for an ensemble averaging, originate from molecules crossing the

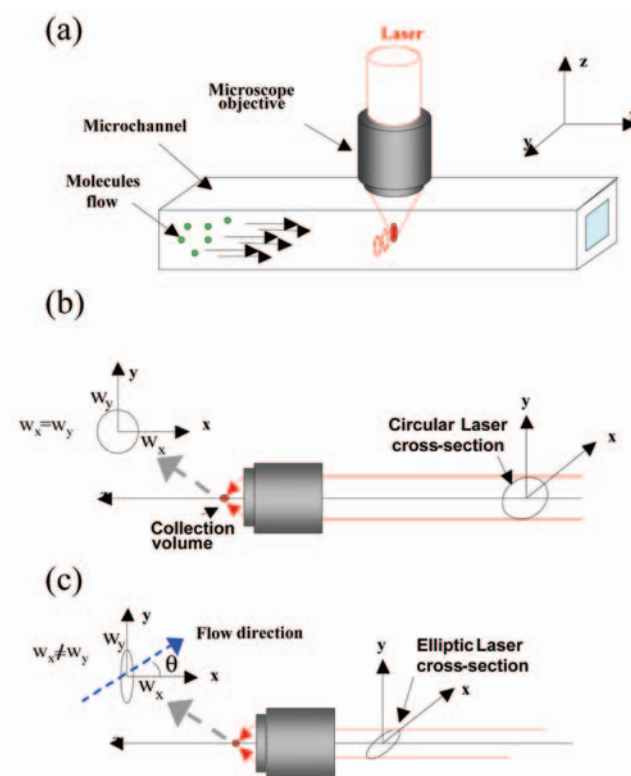


Fig. 1. Schematic view of the FCS set-up for flow velocity profiling. A high numerical aperture objective focalizes the laser beam in the capillary (a). (b) and (c): collection volume cross-sections for a circular and asymmetric laser beam cross-sections, respectively.

collection volume by simple diffusion or flow. Under stationary assumption, the autocorrelation function $g^{(2)}(\tau)$ equals:

$$g^{(2)}(\tau) = \frac{\langle i(t)i(t+\tau) \rangle}{\langle i \rangle^2} = 1 + \frac{\langle \delta i(0)\delta i(\tau) \rangle}{\langle i \rangle^2} \quad (1)$$

Assuming a uniform translation flow along the x direction $V(r) = V_x(y,z)$, Eq. 1 becomes

$$g^{(2)}(\tau) = 1 + \frac{1}{N} \exp\left(-\frac{\tau}{\tau_{flow}}\right)^2 f(\tau) \langle f(\tau) \rangle \quad (2)$$

$$\text{where } f(\tau) = \frac{1}{\left(1 + \frac{\tau}{\tau_d^x}\right)^{1/2} \left(1 + \frac{\tau}{\tau_d^y}\right)^{1/2} \left(1 + \frac{\tau}{\tau_d^z}\right)^{1/2}}$$

Here τ_{flow} is the characteristic time for flow through the collection volume $\tau_{flow} = \frac{2w_x}{V_x(y,z)}$, τ_d^x , τ_d^y and τ_d^z , are the

characteristic times for diffusion in the x , y and z dimensions, respectively: $\tau_d^x = \frac{w_x^2}{4D}$, $\tau_d^y = \frac{w_y^2}{4D}$ and $\tau_d^z = \frac{z_0^2}{16D}$, where D

stands for the translation diffusion coefficient. In our case where z_0 is much larger than w_x and w_y , the two-dimensional model [18] can be applied and $f(\tau)$ simplifies in:

$$f(\tau) = \frac{1}{\left(1 + \frac{\tau}{\tau_d^x}\right)^{1/2} \left(1 + \frac{\tau}{\tau_d^y}\right)^{1/2}}$$

Experimentally (see section 3), we determine τ_d^x , τ_d^y , separately from τ_{flow} by measuring $g^{(2)}(\tau)$ twice: first without flow ($\tau_{flow} \rightarrow \infty$) and then with flow.

Flow Directionality Measurements by FCS

Correlation times are directly related to the dimensions of the collection volume (see Equation 2). The correlation time τ_{flow} increases linearly with the volume dimension along the flow direction but is independent on the volume dimensions in the perpendicular plane. We take benefit of this dependence using an asymmetric volume to determine flow directionality. In conventional FCS, the collection volume is an ellipsoid of revolution about the optical axis. This symmetry is due to the plane transverse cross-section of the laser beam that is circular. Its radius sets the transverse waist $w_p = w_x = w_y$ at the focal plane of the microscope objective. The key element of our method is to modify the transverse beam profile in order to change the transverse aspect ratio $w_x/w_y < 1$.

Let us assume that a flow of speed v is directed along a direction that makes an angle θ with the x axis (See figure 1c). τ_{flow} increases when θ varies from 0 to 90° since the distance in the collection volume over which molecules travel increases. In particular τ_{flow} is minimum when $\theta = 0$. In other words the flow direction is given when the smallest dimension of the collection volume is parallel to the flow. It is therefore possible to determine the flow direction transverse to the optical axis by simply rotating the collection volume about the same axis.

This technique will be implemented and discussed in the last section "Flow directionality measured with FCS".

Hydrodynamic and Electrophoretic Flows

Hydrodynamic Flow

When a pressure difference Δp is applied over a liquid-filled capillary, a stationary flow establishes with a velocity v given by the Hagen-Poiseuille equation:

$$v(y) = \frac{\Delta p}{2\eta L} \cdot \left[\left(\frac{a}{2} \right)^2 - y^2 \right] \quad (3)$$

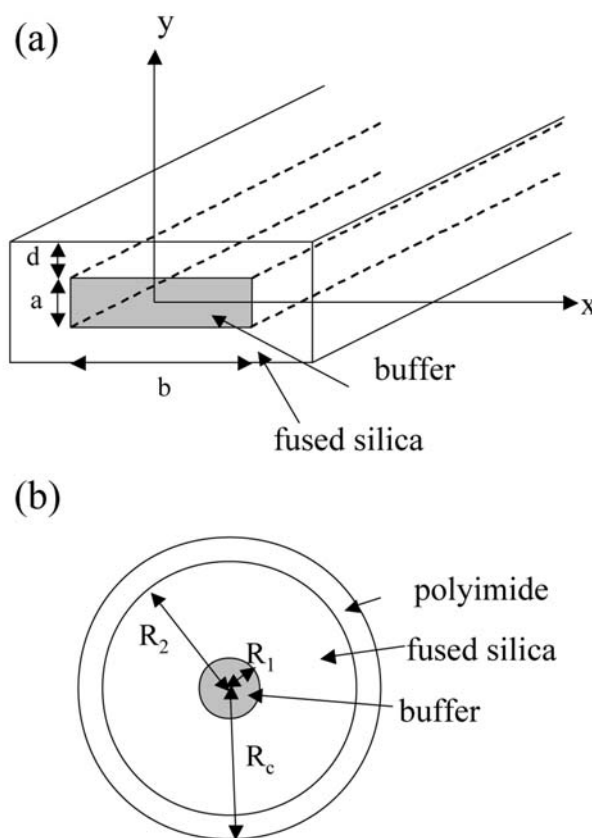


Fig. 2. Microchannel geometries with rectangular (a) and circular (b) cross-sections.

Here, we consider the case of a capillary with a rectangular cross section with one dimension (width noted b) much greater than the other (height noted a) (see Figure 2a). η is the viscosity of the buffer and L the length of the capillary. This equation which is valid for laminar flow (i.e. for low number Reynolds) corresponds to a parabolic velocity profile.

Capillary Electrophoresis and Temperature Effect

An electric field applied over the capillary results in an electrophoretic flow. In all the following calculations we assume that electroosmotic forces are negligible with respect to electrokinetic ones (an assumption which is true in our experiments).

Velocity in a Circular Capillary

The electrokinetic velocity of a charged molecule within a circular capillary can be written as

$$v = \frac{q}{6 \cdot \pi \cdot \eta \cdot r_m} \cdot E, \quad (4)$$

where q is the charge of the molecule, E the electric field strength, η the buffer viscosity and r_m the solute radius. As η depends on temperature T , the velocity profile is also a function of T . Solving the heat conduction equation leads to

$$[19] \quad T(r) = T_1 + \frac{G \cdot R_1}{4 \cdot K_1} \cdot \left(1 - \frac{r^2}{R_1^2}\right), \text{ where } R_1 \text{ is the internal radius}$$

of the capillary (see figure 2b), G the heat generation rate, K_1 the buffer thermal conductivity of and T_1 the temperature at $r=R_1$. T_1 is also determined by solving the heat conduction equation. In this case,

$$T_1 = T_a + \frac{G \cdot R_1^2}{2} \cdot \left[\frac{1}{K_2} \cdot \ln\left(\frac{R_2}{R_1}\right) + \frac{1}{K_C} \cdot \ln\left(\frac{R_C}{R_2}\right) + \frac{1}{R_C \cdot h} \right] \quad (5)$$

where T_a is the ambient temperature, K_2 and K_C are the thermal conductivity of the fused silica and the thermal conductivity of the polyimide coating, respectively, R_2 and R_C are the capillary radii (see figure 2b) and h is the heat transfer coefficient of the surroundings.

Note that G can be calculated with $G = \frac{E \cdot I}{\pi \cdot R_1^2}$,

where I is the electric current in the capillary.

As η is given by

$$\eta = A \cdot \exp\left(\frac{B}{T}\right), \quad (6)$$

where A and B are two constants. Replacing equation (4) and (5) into (6) and using a first order expansion around $T=T_1$, the velocity profile becomes [19]

$$v(r) = v_1 \left[1 + \frac{G \cdot B \cdot R_1^2}{4 \cdot K_1 \cdot T_1^2} \left(1 - \frac{r^2}{R_1^2}\right) \right] \quad (7)$$

where v_1 is the velocity at $R=R_1$, which is a constant term. Eq. 7 shows that non constant velocity profile may appear in capillary electrophoresis. The second term is parabolic and arises from temperature gradient across the capillary.

Velocity Profile in a Rectangular Capillary

In this section we assume that the cross section of the capillary is rectangular. The calculations have been made by considering that b is much greater than a (see figure 2-a). In this case the temperature varies very slowly along axis x with respect to axis y and the problem may be treated in one dimension.

The same method of resolution as the one used in the previous section leads, for $y \leq |a/2|$, to

$$T(y) = T_1 + \frac{G \cdot a^2}{2 \cdot K_1} \cdot \left(-\frac{y^2}{a^2} + \frac{y}{a}\right) \quad (8)$$

where a is the width of the capillary and T_1 is given by

$$T_1 = T_a + \frac{G \cdot a}{2} \cdot \left(\frac{d}{K_2} + \frac{1}{h}\right), \quad (9)$$

where d is the thickness of the capillary (Figure 2b) and G is the heat generated within the capillary. We have

$$G = \Lambda \cdot C_b \cdot E^2, \quad (10)$$

where Λ is the equivalent conductance and C_b is the concentration of the buffer.

Consequently the velocity profile in the capillary can be written as

$$v(y) = v_1 \cdot \left[1 + \frac{G \cdot B \cdot a^2}{2 \cdot K_1 \cdot T_1^2} \cdot \left(-\frac{y^2}{a^2} + \frac{y}{a}\right) \right] \quad (11)$$

where v_1 is the velocity at $y = \pm a/2$. As for circular capillary, a parabolic term is superimposed on the constant term. It relates the electrophoretic velocity to experimental parameters. In particular, its dependence with the size of the capillary is quadratic.

Experiments

Microchannels used in this work are either fused silica cylindrical capillaries (50 μm diameter- Supelco) or rectangular capillaries (section: 100 μm x 2000 μm - Dynamics Inc).

They are glued on glass cover-slips and connected to reservoirs made of cone tips. Channels and reservoirs are filled with low concentration (Cy5-dCTP – Amersham) of Cy5 (10^{-10} M) in ultra-pure water or Tris-borate buffer. For hydrodynamic flow, the sample reservoir is a 10 ml pipette connected to one of the two cone tips. The pipette is held at a height of few cm above the capillary to produce the hydrostatic pressure. For electrophoretic flows, platinum electrodes are inserted in the cone tips to apply an electric field over the capillary.

We use a custom FCS set-up to perform velocity measurements [20]. Flow directionality is determined thanks to a non-symmetric transverse beam profile. Such a beam shape is produced by inserting an adjustable slit into the

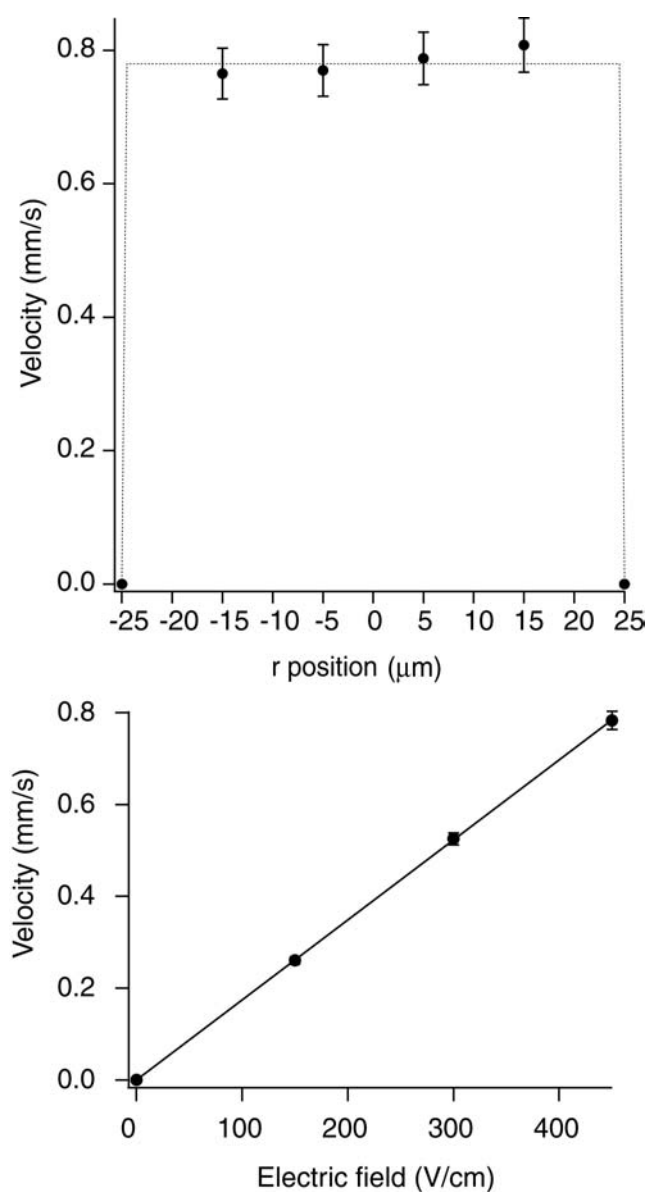


Fig. 3. Velocity profile (a) and electric field strength dependence of the velocity (b) in a circular capillary. Continuous lines represent theoretical velocities given by Eq. 7 using the following parameters: $R_1=25 \mu\text{m}$, $B=2400\text{K}$, $K_1=0.605\text{W}/(\text{m}\cdot\text{K})$, $I=80 \mu\text{A}$, $160 \mu\text{A}$, $I=240 \mu\text{A}$ (for $E=150, 300, 450 \text{ V/cm}$, respectively), $T_1=293\text{K}$, and $v_1=0.26, 0.52, 0.78 \text{ mm/s}$ (for $E=150, 300, 450 \text{ V/cm}$, respectively). With such experimental parameters, the parabolic term is negligible.

He-Ne collimated beam falling on the microscope objective back side.

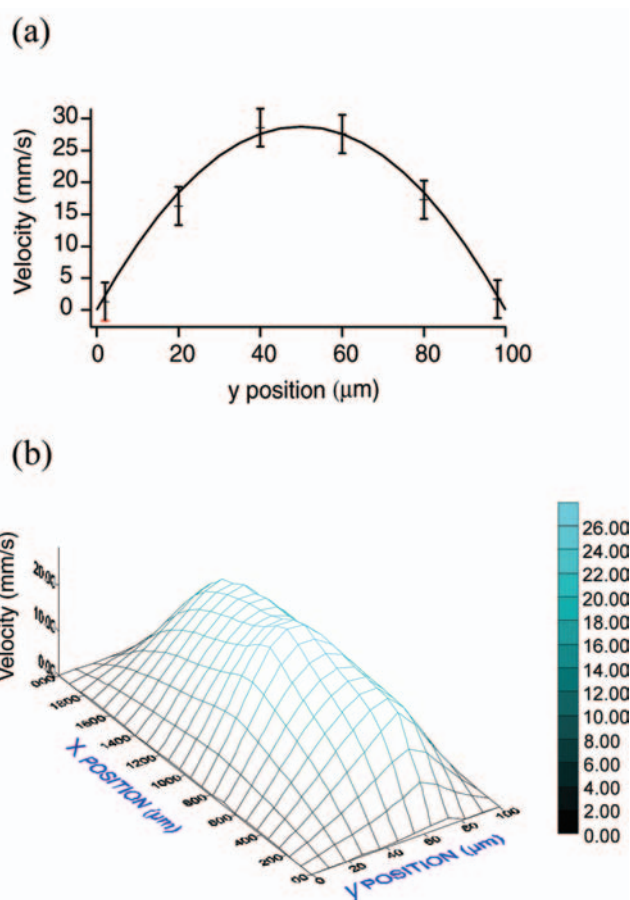


Fig. 4. velocity profile of an hydrodynamic flow. Experimental parameters ($\Delta p=1.323 \times 10^3 \text{ N/m}^2$, $\eta=959 \times 10^{-6} \text{ N}\cdot\text{s/m}^2$, $L=6 \text{ cm}$ and $a=100 \mu\text{m}$) were fixed in the Hagen-Poiseuille equation to calculate the theoretical profile of Eq. 3 (continuous line).

Results and Discussion

Electrophoretic and Hydrodynamic Velocity

Profiles in Small Capillaries

First we calibrate the detection volume by measuring the autocorrelation function for Cy5 (10^{-10} M) in a capillary with no flow. The cross-section of the laser beam is set circular so that $w_x = w_y$ and thus $\tau_d^x = \tau_d^y$. Knowing the diffusion coefficient for Cy5 in water ($D=2.5 \times 10^{-8} \text{ cm}^2/\text{s}$) we deduced from fit $w_x = w_y = 0.5 \mu\text{m}$ (Eq. 2). This value is then fixed in the flow equation (Eq. 2) to determine the velocities of flowing molecules. To establish the velocity profile, we measure the autocorrelation functions at different positions in the microcapillary by moving the capillary holder with respect to the microscope objective. We deduce τ_{flow} from autocorrelation function (ACF) fits and

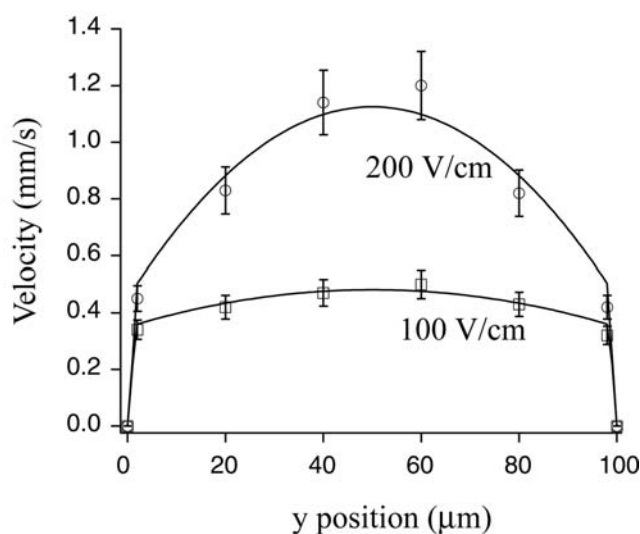


Fig. 5. Electrophoretic flow velocity profile in a rectangular capillary for two different values of the field strength. The theoretical profile shown as a continuous line was calculated from Eq. 11 using the following parameters: $a=0.1$ mm, $B=2400$ K, $C_b=91$ mol/m³, $K_1=0.605$ W/(m.K), $A=0.82$ m²/(Ω .mol) and $T_1=333$ K (T_1 was deduced from Eq. 9).

then the flow velocity from the relation $v = w_x / \tau_{\text{flow}}$. The acquisition time necessary to determine τ_{flow} with a good accuracy is dependent on the velocity: it ranges from few μ s for high velocities (>5 mm/s) to few tens of ms for low velocities flows (<1 mm/s).

Electrophoretic Flow

Figure 3a shows the velocity profile in a 50 μ m diameter circular capillary for Cy5-dCTP molecules driven by an electrophoretic flow. As expected the velocity profile is constant for electrophoretic flow and the velocity increases linearly with the applied electric field (Figure 3b). We found the same velocity value for both horizontal and vertical directions. We are not able to determine the velocity profile in the close vicinity of the capillary surface because the coating of the glass capillary gives rise to a notable background fluorescence signal. Though, the measured profile is flat over the major cross-section of the capillary.

Hydrodynamic flow

For comparison with the previous electrophoretic flow, we measure now the velocity profile of a pressure-driven flow (=hydrodynamic flow) in a 200x2000 μ m² rectangular capillary (see Figure 2-a). For this type of flow (Figure 4-a), the velocity profile is parabolic as predicted by Eq. 3. Figure 4-b shows the whole profile for a cross-section of the rectangular

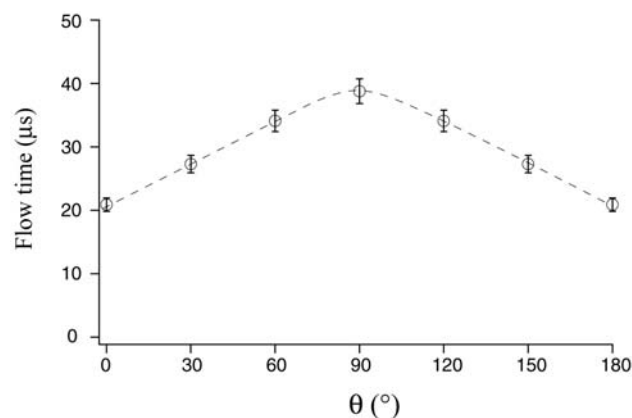


Fig. 6. Flow times τ_{flow} versus the angle θ between the small axis of the laser cross section (at the focal plane) and the flow direction (see fig. 1-c).

capillary. This was extrapolated by two series of measurements along the both cross-section directions. A direct comparison of Fig 3 and 4 shows that flow velocities that can be driven by pressure forces are much higher than those by electrokinetic forces [17].

High flow velocities obtained by hydrodynamic flow are of particular interest for high throughput screening but do not allow the spatial separation of species due to the parabolic transverse velocity profile. In most cases, capillary electrophoresis does not present this drawback; it allows separation of species depending on their charge over mass ratio and the constant velocity profile ensures a constant separation zone. But this advantage falls for large capillaries as demonstrated in the next section.

Electrophoretic Flow in Large Capillary

To address the question of thermal effect in capillary electrophoresis, we measure the velocity profile of Cy5-dCTP molecules electro-kinetically driven in a rectangular capillary with 100x1000 μ m² cross-section. The method follows that presented in the previous section. Figure 5 shows the velocity profile along the y direction (100 μ m wide) for two different applied electrical fields. The profile are not flat, even for low electrical field. We then fit the two different profiles with the expression given by Eq. 11. As predicted by this latter equation, a parabolic term, which is quadratic with the field strength superimposes on the flat velocity term. As explained in the theory section, this effect is the consequence of a buffer viscosity variation over the capillary section. Among the parameters that can produce such an effect, our results demonstrates that the capillary width is an important factor. Use of large capillary widths or radii may cause increased plate heights and lower separation efficiencies in capillary zone

electrophoresis by perturbing velocity profile. Our measurements demonstrate that FCS is a valuable tool to detect effect of temperature gradients with high-resolution.

Flow Directionality Measurements with FCS

In the previous sections, the flow direction was assumed to be directed along the z axis of the capillary. Rather more complicated situations can arise from microfluidics structures that present complex geometries such as curves, crossings and methods that measure flow directions at micron scales are thus required.

For this purpose we break the beam cross-section circular symmetry so that w_x does not equal w_y . To achieve this asymmetric beam, we introduced an adjustable slit in the collimated excitation beam path of our FCS set-up. We call arbitrarily x and y the axis parallel and perpendicular to the slit, respectively. The slit reduces the extension of the transverse beam section in the y direction leading to an increase of w_x (because the objective is under filled in this direction). By this way we can impose $w_x/w_y < 1$. We then rotate the slit about the optical axis in order to change the angle between x and the flow direction. We measured for various angles the correlation function $g^{(2)}(t)$ and determined τ_{flow} by ACF fits with Expression 2. As shown in the Figure 6, τ_{flow} increases when θ varies from 0 to 90°. As expected τ_{flow} is minimum for $\theta=0^\circ$. Although implemented here in a simple capillary geometry, our results demonstrate that our method is able to determine locally the flow direction in a more complex microfluidics structures with non laminar flows. The only requirement being that the velocity variation remains small over the transverse confocal surface ($\pi w_x w_y$).

Conclusion

FCS is a master-tool to determine velocity flow profiles. We have shown that it can be applied successfully not only to measure velocities in different capillaries for hydrodynamic flows [17] but also it appears as an accurate technique to determine electrophoretic flow spatial variation versus applied voltage. Furthermore we have demonstrated that FCS can be used to determine the flow directionality locally with micrometer resolution. FCS will be of particular interest for microfluidic devices which are dedicated to proteins or DNA assays. Our method is indeed still applicable in devices where viscous effects are important and molecules move slowly since the residence time of molecules in the small confocal volume remains relatively short. In the future we expect a large

impact of FCS and related techniques in determining flows in microfluidics structures.

References

- [1] Eigen, M., and Rigler, R., Proc. Natl. Acad. Sci. USA **91** (1994) 5740-5747.
- [2] Goodwin, P. M., Johnson, M. E., Martin, J. C., Ambrose, W. P., Marrone, B. L., Jett, J. H., and Keller, R. A., Nucleic Acids Res. **21** (1993) 803-806.
- [3] Sauer, M., Angerer, B., Ankenbauer, W., Foldes-Papp, Z., Gobel, F., Han, K. T., Rigler, R., Schulz, A., Wolfrum, J., and Zander, C., J. Biotechnol. **86** (2001) 181-201.
- [4] Ma, Y., Shortreed, M. R., Li, H., Huang, W., and Yeung, E. S., Electrophoresis **22** (2001) 421-426.
- [5] Giese, A., Bieschke, J., Eigen, M., and Kretzschmar, H. A., Arch. Virol. Suppl. **16** (2000) 161-171.
- [6] Auer, M., Drug. Discov. Today **6** (2001) 935-936.
- [7] Nie, S., and Zare, R. N., Annu. Rev. Biophys. Biomol. Struct. **26** (1997) 567-596.
- [8] Woolley, A. T., and Mathies, R. A., Proc. Natl. Acad. Sci. USA **91** (1994) 11348-11352.
- [9] Figeys, D., Anal. Chem. May **1** (2000) 330A-335A.
- [10] Simpson, P. C., Roach, D., Woolley, A. T., Thorsen, T., Johnston, R., Sensabaugh, G. F., and Mathies, R. A., Proc. Natl. Acad. Sci. USA **95** (1998) 2256-2261.
- [11] Hess, S. T., Huang, S., Heikal, A. A., and Webb, W. W., Biochemistry **41** (2002) 697-705.
- [12] Zander, C., Drexhage, K. H., Han, K. T., Wolfrum, J., and Sauer, M., Chem. Phys. Lett. **286** (1998) 457-465.
- [13] Kask, P., Palo, K., Ullmann, D., and Gall, K., Proc. Natl. Acad. Sci. USA **96** (1999) 13756-13761.
- [14] Sterrer, S., and Henco, K., J. Recept. Signal. Transduct. Res. **17** (1997) 511-520.
- [15] Winkler, T., Kettling, U., Koltermann, A., and Eigen, M., Proc. Natl. Acad. Sci. USA **96** (1999) 1375-1378.
- [16] Moore, K., Turconi, S., Ashaman, S., Ruediger, M., Haupts, U., Emerick, V., and Pope, J., J. Biomol. Screen. **4** (1999) 335-353.
- [17] Gosch, M., Blom, H., Holm, J., Heino, T., and Rigler, R., Anal. Chem. **72** (2000) 3260-3265.
- [18] Elson, E. L., and Magde, D., Biopolymers **13** (1974) 1-27.
- [19] Grushka, E., Mc Comick, R. M., and Kirkland, J. J., Anal. Chem. **61** (1989) 241-246.
- [20] Begon, C., Rigneault, H., Jonsson, P., and Rarity, J. G., Single Mol. **3** (2000) 207-214.